

**LEACHING OF CEMENT: STUDY OF THE SURFACE LAYER**

**P. Faucon<sup>1,3</sup>, P. Le Bescop<sup>2</sup>, F. Adenot<sup>2</sup>, P. Bonville<sup>1</sup>, J.F. Jacquinot<sup>1</sup>,  
F. Pineau<sup>4</sup> and B. Felix<sup>4</sup>**

<sup>1</sup>Service de Physique de l'Etat Condensé, C.E.A. Saclay, 91191 Gif sur Yvette, France

<sup>2</sup>Service d'Entreposage et de Stockage des Déchets, C.E.A. Saclay, 91191  
Gif sur Yvette, France

<sup>3</sup>Service de Chimie Moléculaire, C.E.A Saclay, 91191 Gif sur Yvette, France

<sup>4</sup>ANDRA, Parc de la Croix Blanche, 1-7 rue Jean Monnet, 92298 Châtenay-Malabry, France

(Refereed)

(Received April 15, 1996; in final form September 3, 1996)

**ABSTRACT**

Leaching of cement pastes shows that the properties of the surface layer are similar whether or not the cement paste contains slag. Substantial amounts of calcium, and smaller amounts of silicon, are leached out. Iron and magnesium are not released, but their content in the surface layer increases, with respect to an internal reference. Magnesium precipitates in the form of hydrotalcite, whereas the calcium of calcium silicate hydrates (CSH) is replaced by iron and dissolves out. Hydrogarnets undergo little, or no, leaching. *Copyright © 1996*

*Elsevier Science Ltd*

**Introduction**

Short-lived, and possibly long-lived, radioactive waste is, or will be, stored in concrete containers (casks, disposal structures, etc.). To predict the safety of these containers, the composition and structure of the material when degraded must be known.

The French Atomic Energy Commission (CEA) has for many years studied the degradation of concrete by leaching with water (1), in order to model its long-term behaviour under worst-case attack conditions (flowing water).

We have studied the leaching with constantly demineralized water of two mineralogically distinct cement pastes: ordinary Portland cement (OPC), and a mixture of OPC (30%) and slag (70%).

Our aim was to characterize the phases formed on contact with demineralized water, and the phases which dissolve, or not, during the water attack. X-ray diffraction was used to study the surface layer, but by its nature could not provide evidence of poorly crystallized or amorphous phases. The presence of calcite in hydrated cement pastes makes identification of CSH by X-ray diffraction difficult since it, like CSH, has a main peak at 0.303 nm.

We therefore completed our study of the degraded layer by Mössbauer spectroscopy on <sup>57</sup>Fe. Mössbauer spectra can be used to measure isomer shifts and quadrupolar splittings. Isomer shifts enable the valency of the iron in each site to be accurately determined. Trivalent iron has an isomer shift with respect to  $\alpha$ -Fe which is always below 1 mm/s. A high

TABLE 1  
Chemical Analysis of Cement Pastes

| % per unit mass<br>( $>0,5\%$ ) | CaO  | SiO <sub>2</sub> | Al <sub>2</sub> O <sub>3</sub> | Fe <sub>2</sub> O <sub>3</sub> | MgO | SO <sub>3</sub> | K <sub>2</sub> O | TiO <sub>2</sub> | Na <sub>2</sub> O | Ignition loss<br>(at 1000°C) |
|---------------------------------|------|------------------|--------------------------------|--------------------------------|-----|-----------------|------------------|------------------|-------------------|------------------------------|
| Sample 1                        | 64.1 | 13.0             | 3.3                            | 2.2                            | 0.4 | 2.0             | 0.1              | 0.20             | 0.1               | 35.5                         |
| Sample 2                        | 31.4 | 19.1             | 7.6                            | 1.0                            | 3.6 | 5.9             | 0.2              | 0.4              | 4.1               | 26.4                         |

isomer shift indicates octahedral bonding of trivalent iron ( $\delta > 0.35$  mm/s), whereas a low isomer shift is typical of tetrahedral iron ( $\delta < 0.2$  mm/s). Further studies are necessary for intermediate values. Quadrupolar splittings depend on the local electric field gradient at the site of iron. For trivalent iron, it is characteristic of the symmetry of the site occupied by the trivalent iron. For divalent iron, it is more a function of the electronic wave function around the nucleus than of the symmetry of the site. The isomer shift and quadrupolar splitting therefore depend only on the valency of the iron and on its local environment. They can be used to identify the various sites of iron in the sound paste and in the degraded layer after water attack. Trivalent iron substitutes for calcium in CSH (2,3,4). Mössbauer spectroscopy is therefore able to demonstrate the presence or absence of CSH in a paste and to identify the environment of iron in the various phases of the paste.

### Experimental Procedure

Two different cement pastes were hydrated at W/C 0.38. Sample 1 was an OPC from the Altkirch factory of Ciments d'Origny containing small quantities of gypsum. Sample 2 was a mixture of OPC and slag (70%), used for stabilization of a radioactive Na<sub>2</sub>SO<sub>4</sub> solution. It was hydrated with the solution of Na<sub>2</sub>SO<sub>4</sub> (25% by weight) and then kept at 120°C in steam for three days. This hydrothermal treatment was performed to consume the Na<sub>2</sub>SO<sub>4</sub> solution. The two pastes were kept for two years in a saturated solution of portlandite, before being subjected to water attack.

The crystallized phases initially present in each of the two pastes were detected by X-ray diffraction (TABLE 2) using a Siemens D500/501 powder diffractometer. One can notice the unusual presence of hydrogarnet in sample 1, which did not undergo any hydrothermal treatment. The small quantities of gypsum in the cement lead to enhance hydration temperature and accelerate hydrogarnet precipitation.

A preliminary <sup>57</sup>Fe Mössbauer spectroscopy study of sample 1 indicated that 34% of the iron was in C<sub>4</sub>AF (4) before leaching. C<sub>4</sub>AF was absent from sample 2 because it was completely hydrated during hydrothermal treatment.

Test pieces were kept at pH 7 in a solution deionized by recirculation through a mixed bed of ion-exchange resins. Tests were performed under an inert atmosphere (N<sub>2</sub>). After six

TABLE 2  
Phases Detected by X-Ray Diffraction in Pastes

| Paste   | Sample 1 | Sample 2 |
|---|----------|----------|
| AF <sub>i</sub> , CH, C <sub>3</sub> (A,F)SH <sub>4</sub> , Calcite | yes      | yes      |
| AF <sub>m</sub> , C <sub>4</sub> AF, C <sub>2</sub> S               | yes      | -        |
| phase U, gehlenite, quartz  | -        | yes      |

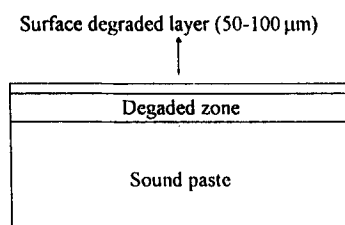


FIG. 1.  
Sample.

months of leaching, the surface degraded layer (thickness 50 to 100 microns) was removed for study by X-ray diffraction spectroscopy, Mössbauer spectroscopy, and chemical analysis (FIG. 1).

The Mössbauer study was performed using a  $^{57}\text{Co}:\text{Rh}$   $\gamma$ -ray source, the spectrometer comprising an electromagnetic vibrator with a triangular velocity signal. All spectra were recorded at ambient temperature. Each sample was exposed to the  $^{57}\text{Co}$  source for about two days. The isomer shifts are given with reference to  $\alpha\text{-Fe}$ . Each spectrum could be decomposed as a sum of lorentzian doublets whose relative intensities, isomer shift, quadrupolar splitting and half-widths (HWHM) were determined using a least square fit procedure. The isomer shifts and the quadrupolar splittings are given to  $\pm 1\%$ . The relative weight of each doublet is given to  $\pm 2\%$ .

## Results

**Chemical analysis.** Chemical analysis (TABLE 3) shows that leaching had similar effects on the two samples.

In both pastes, leaching resulted in a dissolution of calcium. Magnesium and iron were less leached.

**X-Ray Diffraction.** X-ray diffraction spectra of the surface degraded layers of the two samples are shown in FIG. 2. AFm, AFt and portlandite were leached out of the pastes.

Residual anhydrites were seen in the surface layers of the two samples. The first sample contained predominantly  $\text{C}_4\text{AF}$ , whereas the second contained traces of gehlenite and quartz.

Hydrogarnet initially present in both types of pastes was seen in the two surface layers. In sample 1, hydrogarnet gave similar diffraction peaks to those reported by Taylor for  $\text{Ca}_3\text{AlFe}(\text{SiO}_4)(\text{OH})_8$  (5). Comparison of the intensity of the hydrogarnet peaks with those of  $\text{C}_4\text{AF}$  showed that the ratio of peak intensities of the two phases was the same in the sound zone and the surface layer (6). The two phases therefore exhibited similar behaviour. The

TABLE 3  
Ratio of Percentages Per Unit Mass Between Surface Layers and Pastes

| $\frac{\% \text{Surface}}{\% \text{Paste}}$ | CaO | SiO <sub>2</sub> | Al <sub>2</sub> O <sub>3</sub> | Fe <sub>2</sub> O <sub>3</sub> | MgO |
|---|-----|------------------|--------------------------------|--------------------------------|-----|
| Sample 1                                    | 0.5 | 1.0              | 1.9                            | 8.5                            | 7.5 |
| Sample 2                                    | 0.3 | 1.0              | 3.1                            | 5.6                            | 8.8 |

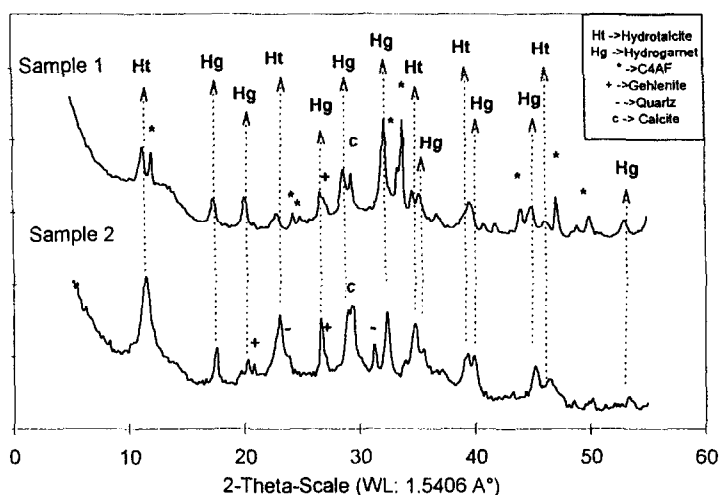


FIG. 2.  
X-ray diffraction spectra of the surface layers.

hydrogarnet of sample 2 gave diffraction peaks corresponding to those reported by Passaglia and Rinaldi (7) for the hydrogarnet, katoite,  $\text{Ca}_3\text{Al}_2(\text{SiO}_4)(\text{OH})_8$ . Hence there was little replacement of aluminum by iron, compared with the hydrogarnet of sample 1.

X-ray diffraction spectra of the two surface layers have a low-intensity peak at 0.303 nm which can be assigned to either CSH or calcite, or both which are present in non-degraded samples.

The precipitation of a new phase was apparent from the X-ray diffraction spectra of the two degraded layers. In OPC, this phase had its main peak at 0.779 nm, which is clearly distinct from the 0.75 nm peak of the AFm of the initial paste. It is perfectly indexed by the diffraction peaks reported by Mascolo and Marino for  $\text{Mg}_6\text{Al}_2(\text{OH})_{18}(\text{H}_2\text{O})_{4.5}$  (8). Non-carbonated hydrotalcite therefore precipitated in the surface layer of the OPC paste. A series of peaks was given by the surface layer of the slag-cement paste, the main peak at 0.773 nm

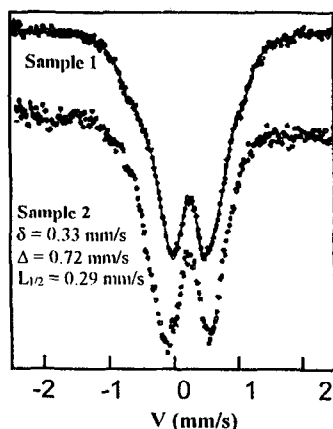


FIG. 3.  
 $^{57}\text{Fe}$  Mössbauer spectra of the superficial layers of the samples ( $V_{\text{max}} = 2 \text{ mm/s}$ ).

TABLE 4  
Characteristics of the  $^{57}\text{Fe}$  Mössbauer Spectrum of the OPC Surface Layer (4)

|                                  | Fe of $\text{C}_4\text{AF}$ | $\text{Fe}_{\text{labile}}$ of the CSH<br>and Fe of $\text{C}_3(\text{A},\text{F})\text{SH}_4$ | $\text{Fe}_{\text{non-labile}}$ of the CSH |
|----------------------------------|-----------------------------|--|--|
| $\delta$ (mm/s), $\Delta$ (mm/s) | 0.34, 1.5                   | 0.39, 0.86   | 0.31, 0.39                                 |
| Half-width: $L_{1/2}$ (mm/s)     | 0.27                        | 0.23   | 0.17                                       |
| Weight of doublet (%)            | 16                          | 53   | 31   |

being broader than in the OPC. Each of the diffraction peaks of the new phase can be flanked by the peaks reported by Koritnig et al (9) for the meixnerite  $\text{Mg}_6\text{Al}_2(\text{OH})_{13}(\text{H}_2\text{O})_4$  and by Jiang (10) for the carbonated hydrotalcite. Slightly carbonated hydrotalcite precipitated in the surface layer of the slag-rich paste, as in OPC, upon attack by demineralized water.

**Mössbauer Spectroscopy on  $^{57}\text{Fe}$ .** The Mössbauer spectrum of the surface layer of sample 1 (FIG. 3, upper part) consists of three doublets with isomer shifts ( $\delta$ ) and quadrupolar splittings ( $\Delta$ ) corresponding to trivalent iron (TABLE 4). The half width of the doublets is characteristic of iron crystallized or nanocrystallized sites. Amorphous phases would have half widths around 0.5 mm/s. The absence of new hydrated iron oxides detected by X-ray diffraction in the surface layer demonstrates that the detected doublets must be attributed only to the iron in the  $\text{C}_4\text{AF}$ , in the CSH and in the hydrogarnet. The doublet with  $\Delta=1.50$  mm/s is attributed to iron in  $\text{C}_4\text{AF}$ (11). As this doublet has a low relative weight (16%), the respective contributions of the octahedral and tetrahedral sites could not be resolved. That is why its half width is relatively high. The doublet with  $\Delta=0.5$  mm/s is attributed to trivalent iron at the octahedral site ( $\delta > 0.35$  mm/s), replacing non-labile calcium of CSH (3, 4). The doublet with  $\Delta=0.90$  mm/s corresponds to the unresolved contribution of trivalent iron at the octahedral site ( $\delta > 0.35$  mm/s), replacing labile calcium of CSH and the aluminum of hydrogarnet (3, 4).

The Mössbauer spectra of sample 2 are shown in FIG. 4: the spectrum of the slag (upper part) consists of a magnetic hyperfine spectrum and of a quadrupolar doublet, of roughly

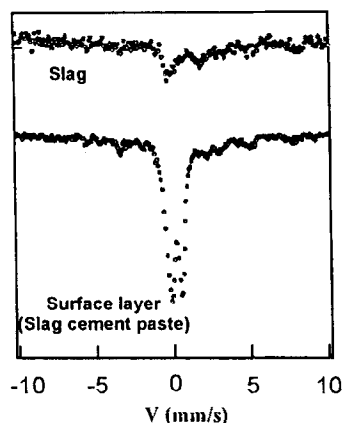


FIG. 4.

$^{57}\text{Fe}$  Mössbauer spectra of sample 2; ( $V_{\text{max}} = 10$  mm/s).

equal intensities; the spectrum of the surface layer (lower part) shows a dominant doublet contribution, and a magnetic hyperfine component. This latter component is very similar to that of the slag, and thus, it corresponds to the presence of undissolved slag in the surface layer. The central part of the surface layer spectrum is reproduced in the lower part of FIG. 3. A precise fit of this spectrum could not be performed because of the presence of the minority slag component; an approximate fit with one quadrupolar doublet yields  $\delta = 0.3$  mm/s and  $\Delta = 0.7$  mm/s. Inspection of the figures in TABLE 4 reveals that this doublet is likely to correspond to the unresolved superposition of labile and non-labile Fe sites in the CSH.

**Quantification of the matrix effect in the OPC.** An element (or a phase) that is not leached may increase in content simply because the other elements dissolve (FIG. 5). In the degraded zone, no  $C_4AF$  dissolution is detected by a quantitative X-ray diffraction study of the OPC degradation (6). After six months of leaching, the concentration per unit volume of  $C_4AF$  in the sound zone is the same as that in the surface layer. We therefore attempted to quantify this "matrix effect" (FIG. 5), using  $C_4AF$  as internal reference.

Let  $m_o$  be the mass of a volume  $dV$  in the sound zone, and  $m$  the mass of the same volume in the surface layer.

Let  $m_{Fo}$  be the mass of  $Fe_2O_3$  in  $dV$  of the sound zone and  $m_F$  the mass of  $Fe_2O_3$  of the surface layer in  $dV$ .

In the sound zone, the %  $Fe_2O_3$  can be written  $2.2\% = 100 \frac{m_{Fo}}{m_o}$  (a)

In the surface layer, this becomes  $18.4\% = 100 \frac{m_F}{m}$  (b)

In the sound paste of the OPC, Mössbauer spectroscopy on  $^{57}Fe$  indicated that 34% of the iron was in the  $C_4AF$ , but that only 16% (TABLE 4) was in the surface layer.

If the mass of iron from  $C_4AF$  in volume  $dV$  is  $m_{Fo}(C_4AF)$  before degradation, and  $m_F(C_4AF)$  after degradation, it is possible to write:

Before attack:  $m_{Fo}(C_4AF) = 0.34 m_{Fo}$

After attack:  $m_F(C_4AF) = 0.16 m_F$

Since  $C_4AF$  is chemically inert (6), its content per unit volume after six months of leaching is the same in the surface layer and in the sound zone. Hence,

$$m_{Fo}(C_4AF) = m_F(C_4AF) \quad \Leftrightarrow \quad 0.34 m_{Fo} = 0.16 m_F$$

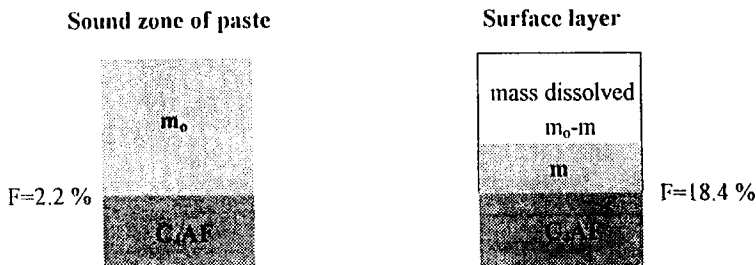


FIG. 5.  
Matrix effect in the OPC sample.

Using (a) and (b) one finds that:

$$\frac{m}{m_o} = 0,25 \text{ (c)}$$

The mass of matter dissolved is therefore

$$100 \frac{(m_o - m)}{m_o} = 75\%$$

To convert the ratios per unit mass of TABLE 3 into ratios per unit volume, one has to correct them by the factor  $\frac{m}{m_o}$ .

The results of TABLE 5 take into account the matrix effect, and show that calcium is the most soluble element. Silica also dissolves, whereas aluminum is less removed. The surface layer is enriched in iron and magnesium. TABLE 5 results take in account the matrix effect. For a constant volume, the rate in iron and magnesium is then twice higher in the superficial degraded zone. If it was a "residual" enrichment, the Fe/Fe<sub>o</sub> and Mg/Mg<sub>o</sub> ratios would be around one. TABLE 5 results demonstrate the migration of these elements to the surface layer, where they accumulate.

### Discussion

Leaching of a cement paste with a demineralized solution creates concentration gradients in the interstitial solution. These gradients result from the diffusion of the ionic species in the degraded zone of the cement paste. The concentrations of the various species of the interstitial solution are modified, resulting in the observed phenomena of dissolution and precipitation.

**Selective Dissolution.** The diffraction spectra of the surface layers indicate that leaching resulted in the disappearance of portlandite, AFm, and Aft. In both types of paste, leaching reduced the calcium concentration in solution to zero in the surface layer. Portlandite, and then AFm and Aft, dissolve, thereby maintaining the calcium concentration of the interstitial solution (12), thus partially explaining the dissolution of 75% of the mass of the surface layer of the OPC.

Leaching of the OPC also resulted in a release of silicon in the aggressive solution (TABLE 5). CSH is the principal phase containing silicon, the removal of which is thus associated with some CSH dissolution. However, iron-substituted CSH is present in the surface layer of the OPC and of the slag-cement. Most of the silicon observed in the surface layer is part of this product.

Leaching reduces the concentrations in solution of all elements to zero in the surface layer. Despite these severe conditions, we noted iron-substituted hydrogarnet in both water-attacked samples. Hydrogarnet, present before degradation, gave strong peak intensities in the surface layers of both samples. In the OPC, the ratio of the intensities of the peaks of C<sub>4</sub>AF to those of hydrogarnet were the same in the paste and in the surface layer. The matrix

TABLE 5  
Elemental Ratios in the Solid Phase after Leaching of an OPC Constant Volume

|                | Ca/Ca <sub>o</sub> | Si/Si <sub>o</sub> | Al/Al <sub>o</sub> | Fe/Fe <sub>o</sub> | Mg/Mg <sub>o</sub> |
|----------------|--------------------|--------------------|--------------------|--------------------|--------------------|
| OPC (sample 1) | 0.1                | 0.3                | 0.5                | 2.1                | 1.9                |

effect is then responsible for the high intensity of the hydrogarnet peaks. In both types of pastes, this phase is little leached.

**Precipitation of Hydrotalcite.** Hydrotalcites are magnesium-containing phases whose structure is derived from that of brucite  $\text{Mg}(\text{OH})_2$  (MH) by substitution of aluminum for magnesium. The charge deficit is compensated by incorporation in the structure of  $\text{OH}^-$  or  $\text{CO}_3^{2-}$  ions (12). Hydrotalcites are characterized by a 0.78 nm peak close to the characteristic peak of the AFm, and have a very similar structure to AFm. The solubility of these phases at near-neutral basic pH is unknown. At pH 8, Atkins *et al.* report for  $\text{M}_6\text{AlH}_{13}$  solubilities of 0.03 mmol/l for Mg and 0.005 mmol/l for Al (13). However, these solubilities are given in the presence of MH, which makes the determination of the dissociation constant of this phase uncertain.

Hydrotalcite, which is poorly soluble at pH's near 7, precipitates in the surface layer of both samples, thus explaining why virtually no magnesium was released in the aggressive solution. The magnesium is initially present in the paste, substituted for calcium in the various phases of the sound paste. Dissolution in the altered layer of part of these phases releases magnesium, which diffuses to the surface where it precipitates in hydrotalcite. The surface layer is thereby enriched in magnesium (TABLE 5).

The hydrotalcite formed is carbonated when calcite is also present in the surface layer. In the surface layer of the OPC, where the calcite was totally dissolved by the water attack, the hydrotalcite was not carbonated. In the cement-slag paste, the surface layer still contained traces of calcite, whose dissolution released  $\text{CO}_3^{2-}$  groups which incorporated in the precipitation process.

**Cationic Substitution in CSH.** In the surface layers of both samples, over 60% of the iron substituted for calcium in the CSH. The Fe/Fe<sub>0</sub> ratio was 2.1 in the OPC. Iron therefore diffused to the surface. In the degraded layer of the OPC, Mössbauer spectroscopy revealed iron in the hydrogarnet,  $\text{C}_4\text{AF}$  and CSH. As the content per unit volume of hydrogarnet and  $\text{C}_4\text{AF}$  did not increase, the iron content of the CSH rose in the surface layer, at the expense of the CSH of the degraded, non-surface zones. The superficial CSH exchanged part of its calcium for trivalent iron ( $\delta < 1$  mm/s). CSH clearly has two sites, one corresponding to the substitution  $\text{Fe}^{3+} \Leftrightarrow \text{Ca}^{2+}_{\text{labile}}$ , and the other to the substitution  $\text{Fe}^{3+} \Leftrightarrow \text{Ca}^{2+}_{\text{non-labile}}$  (3). In the surface layer of the OPC, which is iron-rich ( $\text{Fe}_2\text{O}_3 = 18\%$ , by mass), the two sites are occupied. In the surface layer of the OPC-slag mixture the detection of the  $\text{Fe}^{3+} \Leftrightarrow \text{Ca}^{2+}_{\text{non-labile}}$  substitution is complicated by the presence of magnetic peaks from slag. In the two samples the labile site seems to be the preferred substitution site.

## Conclusions

We have observed the structure of the degraded superficial layer formed when cement pastes are attacked by demineralized water. The properties of the surface layer were comparable, whether or not the initial paste contained slag. These properties are characterized by the presence of residual anhydrides, hydrogarnet little dissolved by the water attack, iron-substituted CSH, and hydrotalcite.

Leaching by demineralized water creates concentration gradients between the surface and the core of the samples. Those gradients change the chemical equilibrium in the interstitial solution of the degraded layer. Portlandite, AFm and Aft phases dissolve. Iron and magne-

sium which substitute calcium and aluminum in these phases pass through the interstitial solution. Then the gradients of concentration in the interstitial solution enhance diffusion of those species to the surface where magnesium precipitates in the form of hydrotalcite, and iron replaces the calcium of CSH.

Leaching of silicon shows that there is partial dissolution of CSH during degradation. However, the high iron content in the surface layer, essentially in CSH, indirectly shows that CSH still predominates in the surface layer. CSH therefore resisted leaching and was characterized by very high cationic substitution rates. This CSH property is related to their structural evolution in degraded zone. Leaching causes indeed a decrease of the calcium concentration in the degraded zone. For low calcium concentration CSH structure is similar to that of tobermorite which has high cationic exchange capacities. These cationic substitutions occurring in CSH during degradation therefore seem to slow down the dissolution of CSH.

The hydrogarnets have particularly slow dissolution kinetics. The partial substitution in  $C_3AH_6$  of  $4OH$  by a  $SiO_4$  may be one of the causes.

### References

1. F. Adenot, Thèse, Université d'Orléans, 1992.
2. H. Stade, K. Ulbricht, H. and Mehner, *Zeit. Anorg Allg. Chem.* **514**, 149 (1984).
3. N.K. Labhasetwar, O.P. Shrivastawa and Y.Y. Medikov, *J. Sol. State. Chem.* **93**, 82 (1991).
4. P. Faucon, P. Bonville, F. Adenot, N. Genand-Riondet, J.F. Jacquinot, J. Virlet, *Advances in Cement Research* (in press).
5. Taylor H., Ingram, University of Aberdeen, Scotland, ICDD, Grant-in-Aid, (1980).
6. P. Faucon, F. Adenot, M. Jorda, and R. Cabrillac, *Materials and Structure* (in press).
7. E. Passaglia and R. Rinaldi, *Bull. Mineral.* **107**, 605 (1984).
8. G. Mascolo and O. Marino, *Min. Mag.* **43**, 619 (1980).
9. S. Koritnig, P. Susse, and Tschermarks, *Mineral. Petrogr. Mitt.* **22**, 79 (1975).
10. S. Jiang, *Aqcta. Mineral. Sinica.* 296 (1984).
11. S. Geller and R.W. Grant and L.D. Fullmer, *J. Phys. Chem. Solids.* **31**, 793 (1970).
12. F. Adenot, and M. Buil, *Cem. Concr. Res.* **22**, 489 (1992).
13. M. Atkins, F.P. Glasser, A. Kindness and D.E. Macphee, DOE Report No DOE/HMIP/RR/91/\*\*\*, Department of the Environment, Aberdeen University (1991).